Systems Studies of Double Null Divertor Models

A.J. Pearce[1], R. Kembleton[2], M. Kovari[1], H. Lux[1], F. Maviglia[2], J. Morris[1], M. Siccinio[2]
1 *United Kingdom Atomic Energy Authority, Culham Centre for Fusion Energy, Culham Science Centre, Abingdon, Oxon, OX14 3DB, UK.*
2 *EUROfusion PMU, Boltzmannstr. 2, 85748 Garching, Germany*

Introduction: An important constraint on future fusion reactor designs are heat exhaust systems, therefore one the crucial components worth the consideration of alternative non-ITER like options is the divertor. One such option is double null (DN) divertor configuration which provides the prospect of improved heat flux management. A systems code models all parts of a fusion power plant and provides consistent solutions allowing for explorations of a large parameter space. The systems code PROCESS [1,2] finds a constrained optimal solution for user specified constraints and figures of merit utilising simple 0D models. The purpose of this study is to employ this systems studies approach to evaluate the interplay of physics and engineering considerations on the suitability of DN configuration for a DEMO power plant.

Model: The magnetic balance is characterised by the flux surfaces of the upper and lower X points and we define the distance between these two flux surfaces at the mid-plane as δR_{sep}. We then define a connected DN configuration as when λ_q, the power decay length in the scrape off layer (SOL), satisfies $|\delta R_{sep}| \leq \lambda_q$ in this scenario the poloidal flux line configuration provides the greatest power load sharing. In a DEMO-like machine it is predicted that λ_q ~ 1mm [3] therefore, operation in the connected DN regime is challenging due to the high degree of control of the plasma needed, due to both the diagnostic systems required and the vertical stabilisation control systems. In addition, the geometry of tokamak devices produces a larger power load onto outer targets, and it has been experimentally shown that operation in DN increases the asymmetry between the inner and outer targets even further [4,5,6]. A DN divertor also introduces new engineering challenges as the addition of a second divertor reduces the area for breeding blankets and will introduce new remote handling considerations possibly reducing availability [7].

The parallel heat flux with the SOL is given by $q_{\parallel} = P_{div}/2\pi \mathrm{R}_0 \lambda_q f_x$ where P_{div} is the power exhausted across the separatrix, R_0 is the major radius, λ_q is the power decay length and the poloidal flux expansion f_x given by $f_x \sim B_p/B$ with B the magnetic field magnitude. Within PROCESS the divertor protection is incorporated by considering a multi-machine scaling relation for the power decay length [3] and taking the limit $B_T \gg B_p$, this process yields the scaling for the divertor protection $P_{sep,max} \sim P_{div} B_T / q_{95} A R_0$ with q_{95} the safety factor, A the aspect ratio and where for DEMO the divertor protection constraint yields

$P_{sep,max}$ = 9.2 MWTm^{-1}. To quantify the degree the upstream power flux is "shared" over the SOL we define the fraction of the power load on the lower divertor targets $f_{div,L}$, therefore we can express the power load to the lower and upper divertor as respectively $P_L = f_{div,L}P_{div}$ and $P_U = (1 - f_{div,L})P_{div}$. This allows for expressing the power imbalance between the divertor regions as $P_z(f_{div,L}) = 2f_{div,L} - 1$. By considering $f_{div,L}$ as an input variable in PROCESS we can explore sensitivity of device designs around the connected DN scenario. Some experiments in machines operating in a DN configuration have shown a decrease in the L-H threshold. We utilise the same scaling as the single null case, as the database is currently not sufficient to derive a DN specific model.

Variable Radial Build: We have performed PROCESS runs with the figure of merit of minimisation of the machine major radius and with the constraint of a minimum net electric power of 500MW and achieving a 2 hour burn time while scanning the upper lower divertor balance P_z. We use the 2018 EU-DEMO baseline for an initial input, allowing for Xe impurities in the SOL as an iteration variable and including a fixed population of W and He impurities. The results of key design parameters from the solution are shown in Fig. 1.

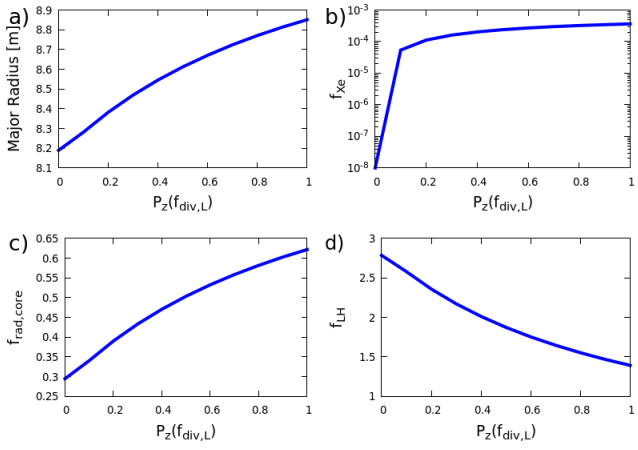

Figure 1. Plots of output variables from PROCESS evaluations while scanning magnetic balance $P_z(f_{div,L})$.

In Fig. 1 we see that in perfectly connected DN we observe significant changes relative to the SN case in crucial power plant design parameters. Fig 1.a shows a reduction in the major radius of the device by ~0.5m due to the improved power load sharing which lowers the constraints on the divertor protection. Another consequence can also be seen in Fig 1.b and Fig 1.c where the fraction of Xenon impurities and the fraction of power radiated in the plasma core decreases. In Fig 1.d we observe a significant increase in f_{LH} showing that a connected DN device is advantageous for safe operation of the plasma in H-mode. We use the SN L-H threshold scaling, but the large increases in P_{sep} allows for a maximum of $f_{LH} = 2.78$

in a balanced magnetic configuration. While these results show promising design improvements, we also note that small changes in the DN configurations magnetic balance can change the optimum solution. Simple estimates would give, for an imbalance parameter $P_z = 0.2$, for example $\delta R_{sep} = 0.4\lambda_q$. For a DEMO like machine with $\lambda_q \sim 1$mm we see that vertical stabilization of a DN magnetic configuration is a challenging task, and there have been recent studies to evaluate the concerns for active and passive stabilisation. [8]

Divertor Target Power Loads: To gain more insight into the power load on the divertor regions we have also studied a simple model describing the power load on each divertor target. We consider both the upper and lower power ratio $f_{div,L}$ and the inner and outer divertor asymmetry f_{io}, with values taken for f_{io} from the EDA H-mode scaling from D. Brunner, *et al* [6]. These values for f_{io} come from studies on Alcator C-Mod and while several engineering and physics parameters differ from that of the current DEMO baseline (e.g. upper open divertor, λ_q and B-field) they provide an estimation to guide future studies. To calculate the power onto each target we also introduce a radiation fraction within the SOL using $P_{tar} = P_{div}(1 - f_{rad,SOL})$ where we use $f_{rad,SOL}$ as an input parameter describing all losses due to impurity and hydrogenic radiation, charge exchange and electron impact ionisation in the SOL.

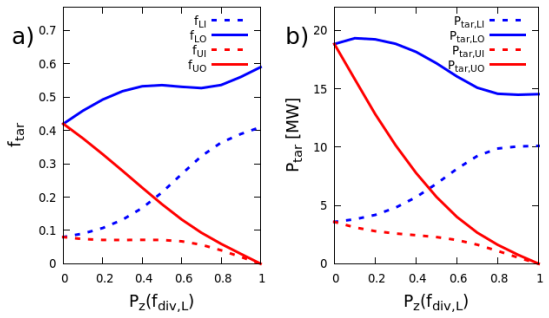

Figure 2. The power balance on the divertor targets, using $f_{rad,SOL} = 0.85$. Panel a) shows fraction of the energy flux f_{tar} to each divertor region a function of the magnetic balance, whereas panel b) shows the magnitude of the power load P_{tar} onto each target. Here the subscripts L and U refer to the lower and upper divertor, while I and O corresponds the inner and outer targets.

In Fig 2.a we observe the larger asymmetries in power fraction f_{tar} to the outer targets in connected DN due to f_{io}. The consequences of the higher inner/outer ratio are seen in Fig 2.b where inner targets are under a reduced load of $P_{tar} = 3.6$ MW. It is suggested that a reduced load on the inner target may allow for its incorporation into the blanket segments [7].

Fixed Radial Build: We have also performed PROCESS runs in which the net electrical power P_{el} is maximised. In these optimisations we have fixed the major radius R_0 at

9.072m as in the 2017 baseline and have required a minimum 2 hour burn time. Fig 3. presents the results of these scans where we have scanned both the peak toroidal field on inboard coil $B_{T,max}$ without the ripple and upper/lower power imbalance P_z.

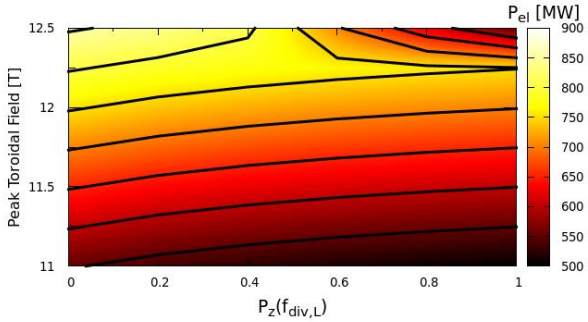

Figure 3. Plot of net electrical power P_{el} as a function of lower/upper power imbalance and the mean peak toroidal magnetic field at the TF coil.

We find that the connected DN increases the power output by ~ 50MW as compared to the SN configuration. Fig 3. also shows that at $P_z(f_{div,L}) > 0.6$ for increasing $B_{T,max}$ there is a decrease in the maximum P_{el}, this non-monotonic behaviour arises due the divertor protection as the large toroidal fields reduce the flux expansion of the flux tubes entering the divertor region and the divertor protection constraint lowers the maximum allowed power over the separatrix. A clear advantage of a connected DN configuration is that this does not occur and so produces much larger improvements relative to SN in P_{el} of around 300MW in the highest B_T regime.

Conclusions: We have explored the DEMO power plant design space with a DN divertor configuration and find improvements in both divertor protection and net generated electrical power, but with additional constraints on plasma control. It would be of interest to test these model present with more complex models of SOL and divertor physics, which could allow for more detailed investigation of inner/outer target power ratio, additionally more study is needed on consequences for other aspects like L-H threshold and remote handing.

This work was funded by the RCUK Energy Programme [grant number EP/P012450/1]. This work has been carried out within the framework of the EUROfusion Consortium and has received funding from the Euratom research and training programme 2014-2018 and 2019-2020 under grant agreement No 633053. The views and opinions expressed herein do not necessarily reflect those of the European Commission.

References

[1] M. Kovari, R. Kemp, H. Lux, P.J. Knight, J. Morris and D.J, Ward, Fusion Eng. Des. **89** 3054-3069 (2014).
[2] M. Kovari *et al*, Fusion Eng. Des. **104** 9-20 (2016).
[3] T. Eich *et al*, Phys. Rev. Lett. **107**, 215001 (2011).
[4] T.W. Petrie *et al*, J. Nucl. Mater. **290,** 935-9 (2001).
[5] G. De Temmerman *et al*, Plasma Phys. Control. Fusion **52**,95005 (2010).
[6] D. Brunner, A.Q. Kuang, B. LaBombardand, J.L Terry, Nucl. Fusion **58**, 076010 (2018).
[7] R. Kemp *et al*, Fusion Eng. Des. **136** 970-974 (2018).
[8] R. Albanese *et al*, Fusion Engineering and Design, https://doi.org/10.1016/j.fusengdes.2019.02.107